Dalton Transactions

ARTICLE

A dipyrromethane-based diphosphane–germylene as precursor to tetrahedral copper(I) and T-shaped silver(I) and gold(I) PGeP pincer complexes†

Received 00th January 20xx,
Accepted 00th January 20xx

DOI: 10.1039/x0xx00000x

www.rsc.org/

Javier A. Cabeza,[a]* Israel Fernández,[b] Pablo García-Álvarez[a] and Carlos J. Laglera-Gándara[a]

A six-membered ring N-heterocyclic germylene flanked by two $CH_2P^iPr_2$ groups, $Ge(pyrmP^iPr_2)_2CMe_2$ (**1**; $(HpyrmP^iPr_2)_2CMe_2$ = 5,5-dimethyl-1,9-bis(di-isopropylphosphanylmethyl)dipyrromethane), has been prepared in high yield. Upon treatment with group 11 metal precursors of the type $[MCl(PPh_3)]_n$ (M = Cu (n = 4), Ag (n = 4), Au (n = 1)), germylene **1** easily forms a PGeP chloridogermyl ligand that is able to stabilize tetrahedral copper(I) and unusual T-shaped silver(I) and gold(I) PGeP pincer complexes, as has been demonstrated by the isolation of $[Cu\{\kappa^3P,Ge,P\text{-}GeCl(pyrmP^iPr_2)_2CMe_2\}(PPh_3)]$ (**2**) and $[M\{\kappa^3P,Ge,P\text{-}GeCl(pyrmP^iPr_2)_2CMe_2\}]$ (M = Ag (**3**), Au (**4**)). Theoretical calculations have shown that the Ge–M bonds of these complexes are weak and that their strength decreases in the series **2** > **3** > **4**.

Introduction

The synthesis and the transition metal (TM) chemistry of bulky and strong electron-donating pincer ligands have attracted much attention in the last decade because many of the resulting metal complexes have been successfully involved in important bond activation and catalytic processes.[1,2]

On the other hand, the heavier analogues of carbenes (heavier tetrylenes, HTs) have been recently recognized as very strong electron-donating ligands[3] and some of their TM complexes have already demonstrated high efficiency in various catalytic reactions.[4,5]

Stimulated by the above-mentioned facts, the incorporation of HTs to pincer ligands has recently started to be investigated. In this field, ECE,[5k,5l,6] ENE,[5d,5h,5i,5j,6d] NEN,[6b,6c] and PEP[7–12] systems (E = Si, Ge or Sn) have already been reported, including some catalytic reactions. Regarding PGeP pincer-type germylenes, we reported the first specimen of this family in 2017 (compound **A**, Fig. 1).[10] Although we managed to prepare some TM complexes with it (compounds of type **A'** in Fig. 1),[13,14] the short length of its $CH_2P^tBu_2$ sidearms resulted in very distorted square geometries for d^8 metal complexes (Rh, Ir, Ni, Pd, Pt) and we failed to isolate any Group 11 metal(I) derivative. Goicoechea's group reported the second PGeP pincer-type germylene in 2018 (compound **B**, Fig. 1) and studied its reactions with Group 11 metal(I) chlorides,[11] but the PGeP germyl ligand of the resulting complexes (compounds of type **B'** in Fig. 1) did not behave as a pincer ligand because the small 5-membered $GeNC_2N$ ring forces a long separation between the P atoms, impeding their binding to the same metal atom. Subsequently, we prepared a very flexible pyrrole-derived PGeP germylene (compound **C**, Fig. 1) that allowed the synthesis of undistorted square-planar d^8 complexes and also a gold(I)

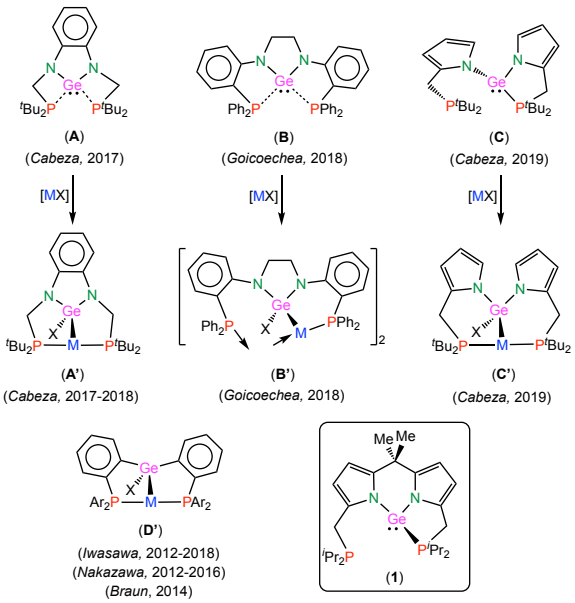

Fig. 1 The currently known PGeP germylenes (**A**–**C**), types of PGeP germyl complexes (**A'**–**D'**; M may be attached to additional ligands) and the new PGeP germylene reported in this work (**1**).

[a]Centro de Innovación en Química Avanzada (ORFEO-CINQA) and Departamento de Química Orgánica e Inorgánica, Universidad de Oviedo, 33071 Oviedo, Spain.
[b]Centro de Innovación en Química Avanzada (ORFEO-CINQA) and Departamento de Química Orgánica I, Facultad de Ciencias Químicas, Universidad Complutense de Madrid, 28040 Madrid, Spain.
*E-mail: jac@uniovi.es (J.A.C.).
†Electronic Supplementary Information (ESI) available: CCDC 1937808–1937811. Detailed experimental, analytical, XRD and DFT data. See DOI: 10.1039/x0xx00000x

derivative (compounds of type **C'** in Fig. 1). However, the germylene itself and its gold complex resulted very unstable toward hydrolysis with adventitious moisture (Cu^{I} and Ag^{I} derivatives could not even be prepared).[12] Most probably, the steric shielding of the Ge atom of **C** (and also of **C'**) is not enough to protect its easily hydrolysable Ge–N bonds. A few TM complexes of type **D'** (Fig. 1) are known, but they have been prepared by oxidative addition of Ge–H or Ge–Cl bonds of $PGe^{IV}P$ ligand precursors to low-valent metal complexes (no group 11 metal derivatives are known).[15,16]

With the above data in mind, we set out the synthesis of the PGeP germylene Ge(pyrmP^{i}Pr$_2$)$_2$CMe$_2$ (**1**; (HpyrmP^{i}Pr$_2$)$_2$CMe$_2$ = 5,5-dimethyl-1,9-bis(di-isopropylphosphanylmethyl)dipyrromethane; Fig. 1), which was expected to be better suited to lead to PGeP pincer complexes than its precedents (germylenes **A**–**C**), because (a) its 6-membered GeNC$_3$N ring would allow a close proximity of the P atoms to the M atom, (b) the CMe$_2$ group bridging both pyrrole rings would offer additional steric protection to the Ge atom (such a bridge is absent in **C**), and (c) the smaller P^{i}Pr$_2$ groups (compared with the P^{t}Bu$_2$ groups of **C**) would modify the reactivity of the TM derivatives (the metal atom is sterically less protected), as has been previously shown for other pincer systems containing PR$_2$ groups (R = ^{t}Bu *vs.* ^{i}Pr).[17]

Results and discussion

Germylene **1** was prepared by treating GeCl$_2$(dioxane) with the dilithiated form of the diphosphane (HpyrmP^{i}Pr$_2$)$_2$CMe$_2$, which was in turn synthesised in two steps from 5,5-dimethyldipyrromethane[18] (Scheme 1) by a synthetic method previously used by Mani's group to prepare other phosphane-functionalized pyrroles and dipyrromethanes.[19]

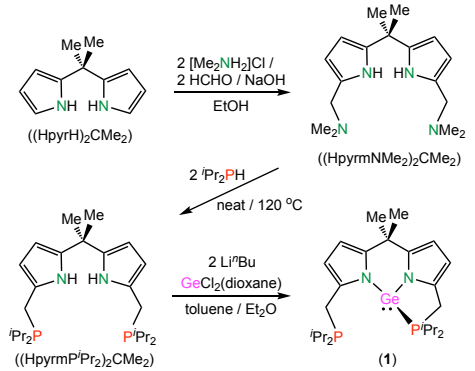

Scheme 1 Synthesis of germylene **1**.

The X-ray diffraction (XRD) structure of germylene **1** (Fig. 2) shows that the Ge atom is in a pyramidal environment attached to both pyrrolyl rings (Ge1–N1 1.950(3), Ge1–N2 1.939(3) Å) and to one phosphane group (Ge1–P1 2.515(1) Å). The remaining phosphane group is far away from the Ge atom (Ge1–P2 3.936(1) Å). The 6-membered GeNC$_3$N ring is folded over the Ge1–C12 line, resulting in a dihedral angle between the pyrrolyl planes of 51.2(1)°. Interestingly, whereas the GeP$_2$N$_2$ atom groupings of germylenes **A**[14] and **B**[11] are almost coplanar, the two pyrrolyl rings of germylene **C** are almost perpendicular to each other, so that one pyrrolyl ring plane actually cuts the other pyrrolyl group into two equivalent halves.[12]

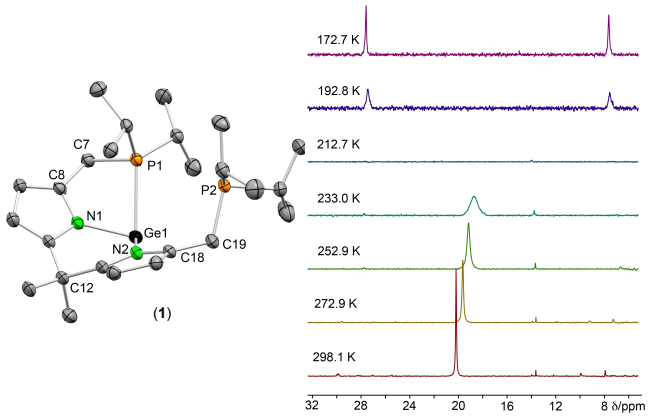

Fig. 2 XRD molecular structure (30% displacement ellipsoids, H atoms omitted for clarity) and VT $^{31}P\{^{1}H\}$ NMR spectra (162.0 MHz, 1/1 toluene/CD_2Cl_2 solution) of germylene **1**.

A view of the frontier molecular orbitals of **1** (ESI, Fig. S24), anticipated an ambiphilic behavior of this molecule, since the Ge lone pair and an empty Ge p orbital are energetically accessible (HOMO–2 and LUMO, respectively).

NMR spectroscopy indicated that germylene **1** is not rigid in solution. At 25 °C, the $^{31}P\{^{1}H\}$ spectrum is a sharp singlet, whereas two separate signals were observed only below –80 °C (Fig. 2). This variable temperature (VT) NMR study confirmed the existence in solution of a dynamic process that exchanges the "free" and the "coordinated" phosphane groups of germylene **1** and that has a very low activation energy, $\Delta G^{\neq}$ (298.15 K) = 8.9 kcal mol^{-1} (line-shape analysis of the VT $^{31}P\{^{1}H\}$ NMR spectra, ESI, Fig. S1 and S2). A similar situation was observed for the related germylene **C**.[12]

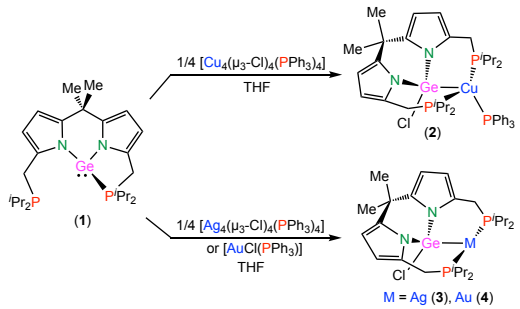

Scheme 2 Synthesis of the PGeP choridogermyl Group 11 metal(I) complexes **2**–**4**.

Germylene **1** reacted readily with [Cu$_4$(μ$_3$-Cl)$_4$(PPh$_3$)$_4$] (1:1/4 mole ratio) in THF at 20 °C to give the PPh$_3$-containing derivative [Cu{κ^3*P*,*Ge*,*P*-GeCl(pyrmP^{i}Pr$_2$)$_2$CMe$_2$}(PPh$_3$)] (**2**; Scheme 2). However, under similar reaction conditions, the silver(I) and gold(I) precursors [Ag$_4$(μ$_3$-Cl)$_4$(PPh$_3$)$_4$] (1:1/4 mole ratio) and [AuCl(PPh$_3$)] (1:1 mole ratio) led to the PPh$_3$-free complexes [M{κ^3*P*,*Ge*,*P*-GeCl(pyrmP^{i}Pr$_2$)$_2$CMe$_2$}] (M = Ag (**3**), Au (**4**); Scheme 2). Complex **4** was more conveniently prepared using [AuCl(THT)] (THT = tetrahydrothiophene) as gold precursor, but intractable mixtures were formed when CuCl and AgCl were

used as metal precursors. In an attempt to remove the PPh_3 ligand of complex **2**, a THF solution was heated at 60 °C for 12 h, but only extensive decomposition was obtained.

The molecular structures of **2**–**4** were determined by XRD (Fig. 3; Table 1). In the three cases, the Ge atom of **1** has inserted into the corresponding M–Cl bond, resulting in a tridentate PGeP chloridogermyl ligand. Interestingly, while the coordination environment of the copper complex **2** is approximately tetrahedral (the Cu atom is also attached to a PPh_3 ligand), that of the silver (**2**) and gold (**3**) complexes is T-shaped (both are isostructural). Therefore, the new dipyrromethane-derived tridentate PGeP germyl ligand is flexible enough to attach a metal atom in either a facial (tripod-type) or meridional (pincer-type) coordination mode. The facial attachment of a PGeP germyl ligand is unprecedented. Noteworthy, the Ge–M distance and the Cl–Ge–M angle of **2**–**4** increase in the series Cu << Ag < Au (Table 1). In comparison with Ge–M (M = Cu, Ag, Au) distances of known complexes containing germyl ligands, the Ge–Cu distance of **2** (2.3580(3) Å) is standard, but the Ge–M distances of **3** and **4** (2.716(1) and 2.7604(4) Å, respectively) are exceptionally long, approximately 0.3 Å longer than the average values reported for such bonds.[20] Additionally, while the Ge atom of **2** features a typical distorted tetrahedral configuration, the environment of the Ge atom of **3** and **4** is better described as distorted trigonal bipyramidal, with the Cl and Au atoms at axial positions and the pyrrolyl N atoms occupying two equatorial sites, hinting to the existence of a lone pair (LP) at the remaining equatorial position.

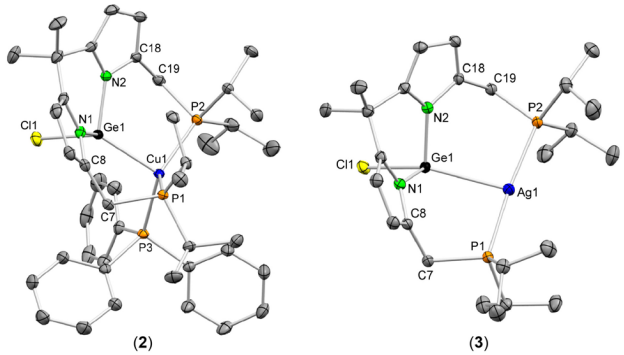

Fig. 3 XRD molecular structures of complexes **2** and **3** (30% displacement ellipsoids, H atoms omitted for clarity). The structure of the gold complex **4** (ESI) is analogous to that of the silver complex **3.**

Table 1 Selected distances (Å) and angles (°) in complexes **2**–**4**.

	2 (M = Cu)	**3** (M = Ag)	**4** (M = Au)
Ge1–M1	2.3580(3)	2.716(1)	2.7604(4)
Ge1–Cl1	2.2631(5)	2.323(1)	2.3534(9)
Ge1–N1	1.903(2)	1.932(3)	1.929(3)
Ge1–N2	1.903(2)	1.921(2)	1.935(3)
M1–P1	2.3267(5)	2.408(1)	2.325(1)
M1–P2	2.3128(5)	2.405(1)	2.3254(9)
Cl1–Ge1–M1	127.87(2)	152.09(3)	155.66(3)
P1–M1–P2	125.60(2)	173.49(3)	175.30(3)

The bonding in complexes **2**–**4** was analyzed by NBO and QTAIM methods (Table 2). The three complexes maintain an almost intact LP on the Ge atom (HOMO–2; ESI, Fig. S25), which is almost aligned with the Ge–M bond in **2** but this is not the case in **3** and **4**. Nevertheless, the LP(Ge) orbitals of **3** and **4**, which have a high s character, do participate in the Ge–M bond, which in the three cases results from a LP(Ge)→σ*(M–P) donation (moderate for Cu and weak for Ag and Cu: $-\Delta E^{(2)}$ = 46.9 (**2**), 32.9 (**3**), 22.8 (**4**) kcal mol^{-1}) coupled with a very weak LP(M)→σ*(Ge–Cl) backdonation ($-\Delta E^{(2)}$ < 5 kcal mol^{-1}) (ESI, Fig. S26). The NBO charges of the Ge and M atoms are both positive in all cases, discarding an attractive electrostatic interaction between these atoms. Accordingly, the Wiberg bond indexes (WBI) of the Ge–M interactions are small and decrease in the series **2** > **3** > **4** (Table 2). The moderate to weak Ge–M interactions indicated by the NBO analysis were confirmed by a QTAIM study (Table 2 and ESI, Fig. S27), which found a small charge density at the corresponding Ge–M bond critical point, (ρ(r)), smaller for **4** than for **3** and **2**). Therefore, the Ge–M bonds of **2**–**4** are weak and their strength decreases in the series **2** > **3** > **4**. All these theoretical data correlate well with the experimental XRD Ge–M bond distances (Table 1). The different Cl–Ge–M angles of **2**–**4** (Table 1) can be rationalized by taking into account that a smaller contribution of the LP(Ge) orbital to the Ge–M bonding implies a greater occupation of the LP(Ge) orbital and a greater repulsion between LP(Ge) and LP(Cl) orbitals, resulting in a wider Cl–Ge–M angle.

Table 2 Theoretical NBO and QTAIM data for complexes **2**–**4**.

	2 (M = Cu)	**3** (M = Ag)	**4** (M = Au)
$-\Delta E^{(2)}$ [LP(Ge)→σ*(M–P)]^a	46.9	32.9	22.8
$-\Delta E^{(2)}$ [LP(M)→σ*(Ge–Cl)]^a	0.6	2.0	4.7
Ge atomic charge^b	+0.77	+0.77	+0.77
M atomic charge^b	+0.78	+0.44	+0.24
$WBI_{Ge–M}$	0.26	0.18	0.14
LP(Ge) occupation^c	1.80	1.87	1.90
$\rho(r_{Ge–M})^d$	0.0646	0.0492	0.0424
$\nabla^2\rho(r_{Ge–M})^e$	0.1123	0.0910	0.0710
$\varepsilon(r_{Ge–M})$	0.0118	0.0910	0.0520

^{a}In Kcal mol^{-1}. ^{b}In au. ^{c}In e. ^{d}In e Å^{-3}. ^{e}In e Å^{-5}.

In solution, the three complexes (**2**–**4**) behave as C_S symmetric molecules, the most significant features of their NMR spectra being the observation of two very broad signals in the $^{31}P\{^1H\}$ spectrum of **2**, due to the quadrupolar nature of ^{63}Cu (69.17 %, I = 3/2), and the presence of two doublets in the $^{31}P\{^1H\}$ spectrum of **3**, due to coupling of the equivalent P nuclei to ^{107}Ag (51.84%, I = 1/2) and ^{109}Ag (48.16%, I = 1/2).

Tetracoordinate copper(I) complexes containing a tridentate ligand are common. However, T-shaped pincer complexes of silver(I) and gold(I) are extremely rare. In fact, as far as we are aware, silver is represented by only one example, a PNP pincer complex,[21] and most of the very few gold complexes[22–24] are derived from PEP pincer Z-ligands (E = Sb,[23] B[24]), which are characterized by an Au→E electron donation.

Conclusions

In summary, a new PGeP germylene, Ge(pyrmP^{i}Pr$_2$)$_2$CMe$_2$ (**1**), based on the dipyrromethane scaffold, has been efficiently prepared. An adequate equilibrium between molecular flexibility and steric protection of the Ge atom makes compound **1** to be better suited for the synthesis of PGeP pincer germyl complexes than the previously known germylenes of this type (compounds **A**–**C**, Fig. 1). In fact, compound **1** has allowed the synthesis of the first mononuclear copper(I) and silver(I) complexes supported by a tridentate PGeP ligand (compounds **2** and **3**) and of an analogous gold(I) complex (compound **4**) that has only one (unstable) precedent.[12] While the cooper complex (**2**) is tetrahedral, the silver (**3**) and gold (**4**) complexes are rare examples of T-shaped pincer derivatives. Theoretical calculations have shown that the Ge–M bonds of these complexes are weak and that their strength decreases in the series **2** > **3** > **4**. No doubt, the successful synthesis of germylene **1** has opened up a new pathway toward PGeP pincer TM complexes for which interesting structural, bonding and catalytic properties can be anticipated.

Experimental section

General data

All reactions and product manipulations were carried out under argon in a drybox or using Schlenk-vacuum line techniques. Solvents were dried over appropriate desiccating reagents and were distilled under argon before use. The compounds (HpyrH)$_2$CMe$_2$,[25] [Cu$_4$(μ_3-Cl)$_4$(PPh$_3$)$_4$],[26] [Ag$_4$(μ_3-Cl)$_4$(PPh$_3$)$_4$][27] and [AuCl(tht)][28] were prepared following published procedures. [AuCl(PPh$_3$)][29] was prepared by treating [AuCl(tht)] with the stoichiometric amount of PPh$_3$. All remaining reagents were purchased from commercial sources and were stored under argon in a drybox. All reaction products were vacuum-dried for several hours prior to being weighted and analyzed. NMR spectra were run on Bruker NAV-400 and AC-300 instruments, using as standards the residual protic solvent resonance for ^{1}H [δ(C*H*Cl$_3$) 7.26 ppm; δ(C$_6$*H*D$_5$) 7.16 ppm; δ(C*H*DCl$_2$) 5.32 ppm], the solvent resonance for ^{13}C [δ(*C*DCl$_3$) 77.16 ppm; δ(*C*$_6$D$_6$) 128.10 ppm; δ(*C*D$_2$Cl$_2$) 54.00 ppm] and external 85% H$_3$PO$_4$ for ^{31}P (δ 0.00 ppm). Microanalyses were obtained with a FlashEA112 (Thermo-Finnigan) microanalyzer. High-resolution mass spectra (HRMS) were obtained with a Bruker Impact II mass spectrometer operating in the ESI-Q-ToF positive mode; data given refer to the most abundant isotopomer of the species with the greatest mass. CHN microanalysis and/or mass spectra were not obtained for the products that were unstable towards air and/or moisture.

Synthetic procedures and characterization data

5,5-Dimethyl-1,9-bis(dimethylaminomethyl)dipyrromethane, (HpyrmNMe$_2$)$_2$CMe$_2$: A solution of (HpyrH)$_2$CMe$_2$ (4.25 g, 24.4 mmol) in ethanol (150 mL) was added to a cold (0 ^{o}C) solution of Me$_2$NH·HCl (4.38 g, 53.7 mmol) in aqueous formaldehyde (4.4 mL of a 37% solution, 53.7 mmol). The resulting solution was allowed to reach the room temperature and was stirred for 3 h. Solid NaOH (2.54 g, 63.4 mmol) was added and the resulting mixture was further stirred for 30 min. A white solid precipitated. The solvent was removed under reduced pressure and the solid residue was extracted into diethyl ether (3 x 30 mL). The combined extracts were dried with anhydrous MgSO$_4$ and the filtered solution was evaporated to dryness to give an orange oil (6.28 g, 89 %). (+)-ESI HRMS: *m/z* 289.2384; calcd. for C$_{17}$H$_{29}$N$_4$ [*M* + H]$^+$: 289.2384. ^{1}H NMR (CDCl$_3$, 300.1 MHz, 298 K): δ 8.08 (br s, 2 N*H*), 5.90 (m, 4 C*H* of pyrroles), 3.31 (s, 4 H, 2 C*H*$_2$NMe$_2$), 2.14 (s, 12 H, 2 N*Me*$_2$), 1.61 (s, 6 H, C*Me*$_2$) ppm. ^{13}C{^{1}H} NMR (CDCl$_3$, 75.5 MHz, 298 K): δ 139.3 (s, *C* of pyrrole), 129.6 (s, *C* of pyrrole), 106.9 (s, *C*H of pyrrole), 103.2 (s, *C*H of pyrrole), 56.8 (s, *C*H$_2$NMe$_2$), 45.1 (s, N*Me*$_2$), 35.5 (s, *C*Me$_2$), 29.3 (s, C*Me*$_2$) ppm.

5,5-Dimethyl-1,9-bis(diisopropylphosphanylmethyl)dipyrromethane, (HpyrmP^{i}Pr$_2$)$_2$CMe$_2$: A thick-walled Schlenk tube equipped with a J. Young manifold was charged with a toluene solution of (HpyrmNMe$_2$)$_2$CMe$_2$ (14.7 mL, 0.55 *M*, 8.0 mmol). The solvent was removed under reduced pressure and neat ^{i}Pr$_2$PH (2.46 g, 20.8 mmol) was added. The tube was immersed in a liquid nitrogen bath and the argon atmosphere was removed under vacuum. The closed tube (under static vacuum) was allowed to reach the room temperature and then it was transferred to an oil bath preheated at 120 ^{o}C. After 24 h, the reaction mixture was allowed to cool down to room temperature and all volatiles were removed under vacuum to give (HpyrmP^{i}Pr$_2$)$_2$CMe$_2$ as an orange oil (3.47 g, 100%). ^{1}H NMR (CDCl$_3$, 300.1 MHz, 298 K): δ 7.72 (br s, 2 H, 2 N*H*), 5.88 (m, 2 C*H* of pyrrole), 5.78 (s, 2 C*H* of pyrrole), 2.69 (s, 4 H, 2 C*H*$_2$P), 1.69 (m, 4 H, 4 C*H*Me$_2$), 1.57 (s, 6 H, C*Me*$_2$), 1.03–0.95 (m, 24 H, 4 CH*Me*$_2$) ppm. ^{13}C{^{1}H} NMR (CDCl$_3$, 75.5 MHz, 298 K): δ 138.2 (s, *C* of pyrrole), 127.9 (d, $J_{C\text{-}P}$ = 7.3 Hz, *C* of pyrrole), 105.8 (s, *C*H of pyrrole), 103.6 (s, *C*H of pyrrole), 35.5 (s, *C*Me$_2$), 29.4 (s, C*Me*$_2$), 23.4 (d, $J_{C\text{-}P}$ = 13.2 Hz, *C*HMe$_2$), 21.0 (d, $J_{C\text{-}P}$ = 19.3 Hz, *C*H$_2$P), 19.8 (d, $J_{C\text{-}P}$ = 14.3 Hz, CH*Me*$_2$), 18.7 (d, $J_{C\text{-}P}$ = 9.2 Hz, CH*Me*$_2$) ppm. ^{31}P{^{1}H} NMR (CDCl$_3$, 121.5 MHz, 298 K): δ 1.2 (s) ppm.

Ge(pyrmP^{i}Pr$_2$)$_2$CMe$_2$ (1): A hexane solution of Li^{n}Bu (3.20 mL, 1.6 *M*, 5.12 mmol) was dropwise added to a cold (–78 ºC) Schlenk tube containing diethyl ether (2 mL) and a toluene solution of (HpyrmP^{i}Pr$_2$)$_2$CMe$_2$ (6.30 mL, 0.37 *M*, 2.33 mmol). The resulting dark orange solution was allowed to reach the room temperature and was stirred for 18 h. The Schlenk tube was then transferred to a drybox. Solid GeCl$_2$(dioxane) (0.533 g, 2.30 mmol) was added and the resulting orange suspension was stirred for 18 h. Solvents were removed under vacuum and the residue was extracted into toluene (3 x 10 mL; solution decanted). The combined toluene extractions were evaporated to dryness. The resulting pale orange oil was crystallized from hexane at –20 ^{o}C to give germylene **1** as colorless crystals (0.962 g, 83 %). ^{1}H NMR (C$_6$D$_6$, 300.1 MHz, 298 K): 6.29 (s, 2 C*H* of pyrrole), 6.21 (s, 2 C*H* of pyrrole), 2.85 (s, 4 H, 2 C*H*$_2$P), 1.86 (s, 6 H, C*Me*$_2$), 1.74–1.62 (m, 4 H, 4 C*H*Me$_2$), 0.92–0.80 (m, 24 H, 4 CH*Me*$_2$) ppm. ^{13}C{^{1}H} NMR (C$_6$D$_6$, 100.6 MHz, 298 K): δ 143.8 (s, *C* of pyrrole), 130.2 (d, $J_{C\text{-}P}$ = 4.3 Hz, *C* of pyrrole), 107.2 (d, $J_{C\text{-}P}$ = 3.8 Hz, *C*H of pyrrole), 103.5 (s, *C*H of pyrrole), 37.1 (s, C*Me*$_2$),

29.6 (s, *C*Me$_2$), 24.2 (br d, $J_{C\text{-}P}$ = 7.3 Hz, *C*HMe$_2$), 22.1 (br s, *C*H$_2$P), 19.1 (d, $J_{C\text{-}P}$ = 7.5 Hz, CH*Me*$_2$), 18.6 (m, CH*Me*$_2$) ppm. ^{31}P{^{1}H} NMR (C_6D_6, 121.5 MHz, 298 K): δ 18.84 (s) ppm.

Variable temperature ^{1}P{^{1}H} NMR study of germylene 1 and line-shape data analysis: A J. Young-stopped NMR tube was charged under argon with germylene **1** (10 mg), toluene (0.2 mL) and dichloromethane-D_2 (0.2 mL) and the resulting solution was analyzed by ^{1}P{^{1}H} NMR at different temperatures (in the range 173–298 K; Fig. S1 of ESI). The corresponding exchange constants (*k*) were obtained by simulation of the experimental spectra with DNMR3[30] (implemented in SPINWORKS[31]). An Eyring plot (Fig. S2 of ESI) afforded the following activation parameters for the exchange process: $\Delta G^{\#}$ (298.15 K) = 8.86 kcal mol^{-1}, $\Delta H^{\#}$ = 8.27 kcal mol^{-1}, $\Delta S^{\#}$ = –1.98 cal K^{-1} mol^{-1}.

[Cu{κ^3*P*,*Ge*,*P*-GeCl(pyrmP^{i}Pr$_2$)$_2$CMe$_2$}(PPh$_3$)] (2): Germylene **1** (0.041 g, 0.08 mmol) was added to a solution of [Cu$_4$(μ$_3$-Cl)$_4$(PPh$_3$)$_4$] (0.029 g, 0.02 mmol) in THF (4 mL). After stirring for 12 h, the solvent was removed under reduced pressure and the residue was washed with 1/1 hexane/diethyl ether (3 x 2 mL) to give complex **2** as a pale violet solid (0.039 g, 55 %). Anal. (%) Calcd. for $C_{43}H_{57}ClCuGeN_2P_3$ (MW = 866.48 amu): C, 59.60; H, 6.63; N, 3.23; found: C, 59.77; H, 6.71; N, 3.17. (+)-ESI HRMS: *m/z* 735.1475; calcd. for $C_{31}H_{47}ClCuGeN_2NaP_3$ [*M* – 2 Ph + Na]$^+$: 735.0146. ^{1}H NMR (CD_2Cl_2, 400.5 MHz, 298 K): 7.53 (m, 6 H of 3 Ph), 7.40 (m, 9 H of 3 Ph), 5.93 (d, $J_{H\text{-}H}$ = 3.1 Hz, 2 C*H* of pyrrole), 5.79 (d, $J_{H\text{-}H}$ = 3.1 Hz, 2 C*H* of pyrrole), 3.12 (m, 2 H of 2 C*H*$_2$P), 3.01 (dd, $J_{H\text{-}H}$ = 12.6 Hz, $J_{H\text{-}P}$ = 4.0 Hz, 2 H of 2 C*H*$_2$P), 1.83 (m, 2 H of 2 C*H*Me$_2$), 1.79 (s, 3 H of C*Me*$_2$), 1.68 (m, 2 H of 2 C*H*Me$_2$), 1.65 (s, 3 H of C*Me*$_2$), 1.08 (dd, $J_{H\text{-}P}$ = 12.6 Hz, $J_{H\text{-}H}$ = 7.2 Hz, 6 H, 2 C*H*$_3$ of CH*Me*$_2$), 0.83 (m, 12 H, 4 C*H*$_3$ of CH*Me*$_2$), 0.48 (dd, $J_{H\text{-}P}$ = 12.6 Hz, $J_{H\text{-}H}$ = 7.2 Hz, 6 H, 2 C*H*$_3$ of CH*Me*$_2$) ppm. ^{13}C{^{1}H} NMR (CD_2Cl_2, 100.6 MHz, 298 K): δ 145.2 (s, *C* of pyrrole), 134.8 (s, *C*H of Ph), 134.6 (s, *C*H of Ph), 130.4 (s, *C*H of Ph), 129.2 (d, $J_{C\text{-}P}$ = 8 Hz, *C* of Ph), 128.9 (s, *C* of pyrrole), 109.3 (s, 1 *C*H of pyrrole), 103.7 (s, *C*H of pyrrole), 37.1 (s, *C*Me$_2$), 35.4 (s, *C*H$_3$ of C*Me*$_2$), 28.9 (s, *C*H$_3$ of C*Me*$_2$), 26.7 (s, *C*H of *C*HMe$_2$), 25.7 (vt, $J_{C\text{-}P}$ = 9.1 Hz, *C*H$_2$P), 24.0 (s, *C*H of *C*HMe$_2$), 19.5 (s, *C*H$_3$ of CH*Me*$_2$), 19.2 (s, *C*H$_3$ of CH*Me*$_2$), 19.1 (s, *C*H$_3$ of CH*Me*$_2$), 17.3 (s, *C*H$_3$ of CH*Me*$_2$) ppm.^{31}P{^{1}H} NMR (CD_2Cl_2, 162.1 MHz, 298 K): δ 10.8 (br s, 2 P), 4.4 (vbr s, 1 P) ppm.

[Ag{κ^3*P*,*Ge*,*P*-GeCl(pyrmP^{i}Pr$_2$)$_2$CMe$_2$}] (3): Germylene **1** (0.041 g, 0.08 mmol) was added to a solution of [Ag$_4$(μ$_3$-Cl)$_4$(PPh$_3$)$_4$] (0.032 g, 0.02 mmol) in THF (4 mL). After stirring for 12 h, the solvent was removed under reduced pressure and the residue was washed with 1/1 hexane/diethyl ether (4 x 2 mL) to give complex **3** as a pale beige solid (0.024 g, 46%). Anal. (%) Calcd. for $C_{25}H_{42}AgClGeN_2P_2$ (MW = 648.51 amu): C, 46.30; H, 6.53; N, 4.32; found: C, 46.42; H, 6.71; N, 4.18. (+)-ESI HRMS: *m/z* 649.0907; calcd. for $C_{25}H_{43}AgClGeN_2P_2$ [*M* + H]$^+$: 649.0856. ^{1}H NMR (CD_2Cl_2, 400.5 MHz, 298 K): 5.95 (d, $J_{H\text{-}H}$ = 2.8 Hz, 2 C*H* of pyrrole), 5.88 (d, $J_{H\text{-}H}$ = 2.8 Hz, 2 C*H* of pyrrole), 3.60–3.35 (m, 4 H of 2 C*H*$_2$P), 2.18 (m, 2 H of 2 C*H*Me$_2$), 1.94 (m, 2 H of 2 C*H*Me$_2$), 1.72 (s, 3 H of C*Me*$_2$), 1.64 (s, 3 H of C*Me*$_2$), 1.26 (m, 12 H, 4 C*H*$_3$ of CH*Me*$_2$), 1.03 (m, 12 H, 4 C*H*$_3$ of CH*Me*$_2$) ppm. ^{13}C{^{1}H} NMR (CD_2Cl_2, 100.6 MHz, 298 K): δ 145.7 (s, *C* of pyrrole), 127.4 (s, *C* of pyrrole), 109.6 (s, *C*H of pyrrole), 104.0 (s, *C*H of pyrrole), 37.3 (s, *C*Me$_2$), 36.2 (s, *C*H$_3$ of C*Me*$_2$), 28.6 (s, *C*H$_3$ of C*Me*$_2$), 25.0 (vt, $J_{C\text{-}P}$ = 10.0 Hz, *C*H$_2$P), 24.1 (m, *C*HMe$_2$), 23.1 (m, *C*HMe$_2$), 21.2 (s, *C*H$_3$ of CH*Me*$_2$), 20.8 (s, *C*H$_3$ of CH*Me*$_2$), 19.9 (s, *C*H$_3$ of CH*Me*$_2$), 17.9 (s, *C*H$_3$ of CH*Me*$_2$) ppm. ^{31}P{^{1}H} NMR (CD_2Cl_2, 162.1 MHz, 298 K): δ 34.9 (2 d, $J_{P\text{-}101Ag}$ = 498 Hz, $J_{P\text{-}107Ag}$ = 433 Hz) ppm.

[Au{κ^3*P*,*Ge*,*P*-GeCl(pyrmP^{i}Pr$_2$)$_2$CMe$_2$}] (4): *Method (a)*: THF (4 mL) was added to a mixture of germylene **1** (0.041 g, 0.08 mmol) and [AuCl(PPh$_3$)] (0.040 g, 0.08 mmol). The resulting orange solution was stirred for 12 h. The reaction mixture was vacuum-dried to give a sticky precipitate, which was washed with hexane (4 x 2 mL) to give **4** as a pale brown solid (0.037 g, 63 %). *Method (b)*: Germylene **1** (0.041 g, 0.08 mmol) was added to a suspension of [AuCl(tht)] (0.026 g, 0.08 mmol) in THF (4 mL). The resulting orange solution was stirred at room temperature for 12 h. The solvent was removed under reduced pressure and the residue was washed with hexane (2 x 2 mL) to give **4** as a pale brown solid (0.049 g, 83 %). Anal. (%) Calcd. for $C_{25}H_{42}AuClGeN_2P_2$ (MW = 737.61 amu): C, 40.71; H, 5.74; N, 3.80; found: C, 40.75; H, 5.79; N, 3.72. (+)-ESI HRMS: *m/z* 703.1748; calcd. for $C_{25}H_{42}AuGeN_2P_2$ [*M* – Cl]$^+$: 703.1706. ^{1}H NMR (CD_2Cl_2, 300.1 MHz, 298 K): 5.99 (d, $J_{H\text{-}H}$ = 3.0 Hz, 2 C*H* of pyrrole), 5.90 (br s, 2 C*H* of pyrrole), 3.89 (d, $J_{H\text{-}H}$ = 14.6 Hz, 2 H of 2 C*H*$_2$P), 3.61 (d, $J_{H\text{-}H}$ = 14.6 Hz, 2 H of 2 C*H*$_2$P), 2.43 (m, 2 H of 2 C*H*Me$_2$), 2.08 (m, 2 H of 2 C*H*Me$_2$), 1.75 (s, 3 H of C*Me*$_2$), 1.64 (s, 3 H of C*Me*$_2$), 1.32 (m, 12 H, 6 C*H*$_3$ of CH*Me*$_2$), 1.05 (m, 12 H, 6 C*H*$_3$ of CH*Me*$_2$) ppm. ^{13}C{^{1}H} NMR (CD_2Cl_2, 100.6 MHz, 298 K): δ 146.2 (s, *C* of pyrrole), 126.0 (s, *C* of pyrrole), 109.7 (s, *C*H of pyrrole), 103.9 (s, *C*H of pyrrole), 37.4 (s, *C*Me$_2$), 35.9 (s, *C*H$_3$ of C*Me*$_2$), 29.0 (s, *C*H$_3$ of C*Me*$_2$), 26.2 (vt, $J_{C\text{-}P}$ = 14.6 Hz, *C*H$_2$P), 25.3 (vt, $J_{C\text{-}P}$ = 11.8 Hz, *C*HMe$_2$), 24.6 (vt, $J_{C\text{-}P}$ = 11.8 Hz, *C*HMe$_2$), 20.3 (s, *C*H$_3$ of CH*Me*$_2$), 20.1 (s, *C*H$_3$ of CH*Me*$_2$), 19.5 (s, *C*H$_3$ of CH*Me*$_2$), 18.0 (s, *C*H$_3$ of CH*Me*$_2$) ppm.^{31}P{^{1}H} NMR (CD_2Cl_2, 121.5MHz, 298 K): δ 60.4 (s) ppm.

Computational details

Geometry optimizations were performed without symmetry constraints using the Gaussian09[32] suite of programs at the BP86[33]/def2-SVP[34] level of theory using the D3 dispersion correction suggested by Grimme et al.[35] This level is denoted BP86-D3/def2-SVP. All species discussed in the text were also characterized by frequency calculations and have positive definite Hessian matrices thus confirming that the computed structures are minima on the potential energy surface. Wiberg Bond Indices (WBIs) and donor-acceptor interactions were computed using the natural bond orbital (NBO6)[36] method. The energies associated with these two-electron interactions have been computed according to the following equation:

$$\Delta E^{(2)}_{\phi\phi^*} = -n_\phi \frac{\langle \phi^* | \hat{F} | \phi \rangle^2}{\varepsilon_{\phi^*} - \varepsilon_\phi}$$

where *F* is the DFT equivalent of the Fock operator and ϕ and ϕ^* are two filled and unfilled Natural Bond Orbitals having ε_ϕ and $\varepsilon_{\phi*}$ energies, respectively; n_ϕ stands for the occupation number of the filled orbital. All QTAIM results described in this

work correspond to calculations performed at the BP86-D3/6-31+G(d)/WTBS(for transition metals) level on the optimized geometries obtained at the BP86-D3/def2-SVP level. The WTBS (well-tempered basis sets)[37] have been recommended for AIM calculations involving transition metals.[38] The topology of the electron density was conducted using the AIMAll program package.[39]

X-Ray diffraction analyses

Crystals of **1**, **2**, **3**·CD_2Cl_2 and **4**·CH_2Cl_2 were analyzed by X-ray diffraction. A selection of crystal, measurement and refinement data is given in Table S1. Diffraction data were collected on an Oxford Diffraction Xcalibur Ruby Geminy (**1**, **2** and **3**·CD_2Cl_2; CuKα radiation) and a Bruker D8 Venture Photon III-14 (**4**·CH_2Cl_2; MoKα radiation) single crystal diffractometers. Empirical absorption corrections were applied using the SCALE3 ABSPACK algorithm (as implemented in CrysAlisPro RED[40]) (**1**, **2** and **3**·CD_2Cl_2) and SADABS-2016/2[41] (**4**·CH_2Cl_2). The structures were solved using SIR-97.[42] Isotropic and full matrix anisotropic least square refinements were carried out using SHELXL.[43] All non-H atoms were refined anisotropically. H and D atoms were set in calculated positions and were refined riding on their parent atoms. The WINGX program system[44] was used throughout the structure determinations. The molecular plots were made with MERCURY.[45]

Conflicts of interest

There are no conflicts to declare.

Acknowledgements

This work was supported by MINECO-FEDER projects CTQ2016-75218-P, CTQ2016-78205-P and CTQ2016-81797-REDC.

References

1 Selected recent reviews on pincer complexes and their applications: (*a*) E. Peris and R. H. Crabtree, *Chem. Soc. Rev.*, 2018, **47**, 1959; (*b*) *The Privileged Pincer–Metal Platform: Coordination Chemistry & Applications*, ed. G. van Koten and R. A. Gossage, Springer, Cham, 2016; (*c*) M. Asay and D. Morales-Morales, *Dalton Trans.*, 2015, **44**, 17432; (*d*) C. Gunanathan and D. Milstein, *Chem. Rev.*, 2014, **114**, 12024; (*e*) *The Chemistry of Pincer Compounds*, ed. K. J. Szabó and O. F. Wendt, Wiley-VCH, Weinheim, 2014; (*f*) *Organometallic Pincer Chemistry*, ed. G. van Koten and D. Milstein, Springer, Heidelberg, 2013.

2 Selected reviews on pincer complexes in homogeneous catalysis: (*a*) G. Bauer and X. Hu, *Inorg. Chem. Front.,* 2016, **3**, 741; (*b*) H. A. Yonus, W. Su, N. Ahmad, S. Chen and F. Verpoort, *Adv. Synth. Catal.*, 2015, **357**, 283; (c) *Catalysis by Pincer Complexes: Applications in Organic Synthesis and Catalysis*, ed. K. J. Szabó and O. F. Wendt, Viley-VCH, Weinheim, 2014; (*d*) Q.-H. Dend, R. L. Melen and L. H. Gade, *Acc. Chem. Res.*, 2014, **47**, 3162.

3 (*a*) Z. Benedek and T. Szilvási, *Organometallics*, 2017, **36**, 1591; (*b*) A. Rosas-Sánchez, I. Alvarado-Beltrán, A. Baceiredo, N. Saffon-Merceron, S. Massou, V. Ranchadell and T. Kato, *Angew. Chem. Int. Ed.*, 2017, **56**, 10549; (*c*) Z. Benedek and T. Szilvási, *RSC Adv.* **2015**, *5*, 5077; (*d*) L. Álvarez-Rodríguez, J. A. Cabeza, P. García-Álvarez and D. Polo, *Coord. Chem. Rev.*, 2015, **300**, 1; (*e*) G. Tan, S. Enthaler, S. Inoue, B. Blom and M. Driess, *Angew. Chem. Int. Ed.*, 2015, **54**, 2214; (*f*) L. Álvarez-Rodríguez, J. A. Cabeza, P. García-Álvarez, E. Pérez-Carreño and D. Polo, *Inorg. Chem.*, **2015**, *54*, 2983; (*g*) J. A. Cabeza, P. García-Álvarez, E. Pérez-Carreño and D. Polo, *Chem. Eur. J.,* 2014, **20**, 8654.

4 For silylene TM complexes in catalysis, see: Y.-P. Zhou and M. Driess, *Angew. Chem. Int. Ed.,* 2018, **58**, 3715.

5 See, for example: (*a*) Y.-P. Zhou, Z. Mo, M.-P. Luecke and M. Driess, *Chem. Eur. J.,* 2018, **24**, 4780; (*b*) J. A. Cabeza, P. García-Álvarez and L. González-Álvarez, *Chem. Commun.*, 2017, **53**, 10275; (*c*) T. Iimura, N. Akasaka, T. Kosai and T. Iwamoto, 2017, **46**, 8868; (*d*) H. Ren, Y.-P. Zhou, Y. Bai, C. Cui and M. Driess, *Chem. Eur. J.,* 2017, **23**, 5663; (*e*) Iimura, N. Akasaka and T. Iwamoto, 2016, **35**, 4071; (*f*) Y. Wu, C. Shan, Y. Sun, P. Chen, J. Ying, J. Zhu, L. Liu and Y. Zhao, *Chem. Commun.,* 2016, **52**, 13799; (*g*) L. Álvarez-Rodríguez, J. A. Cabeza, J. M Fernández-Colinas, P. García-Álvarez and D. Polo, *Organometallics*, 2016, **35**, 2516; (*h*) Y.-P. Zhou, M. Karni, S. Yao, Y. Apeloig and M. Driess, *Angew. Chem. Int. Ed.*, 2016, **55**, 15096; (*i*) Y.-P. Zhou, S. Raoufmoghaddam, T. Szilvási and M. Driess, *Angew. Chem. Int. Ed.*, 2016, **55**, 12868; (*j*) T. T. Metsänen, D. Gallego, T. Szilvási, M. Driess and M. Oestreich, *Chem. Sci.*, 2015, **6**, 7143; (*k*) D. Gallego, S. Inoue, B. Blom and M. Driess, *Organometallics*, 2014, **33**, 6885; (*l*) D. Gallego, A. Brück, E. Irran, F. Meier, F. Kaupp and M. Driess, *J. Am. Chem. Soc.*, 2013, **135**, 15617; (*m*) A. Brück, D. Gallego, W. Wang, E. Irran, M. Driess and J. F. Hartwig, *Angew. Chem. Int. Ed.*, 2012, **51**, 11478.

6 (*a*) W. Wang, S. Inoue, E. Irran and M. Driess, *Angew. Chem. Int. Ed.*, 2012, **51**, 3691; (*b*) F. E. Hahn, L. Wittenbecher, M. Kühn, T. Lügger and R. Fröhlich, *J. Organomet. Chem.,* 2001, **617–618**, 629; (*c*) F. E. Hahn, L. Wittenbecher, D. Le Van and A. V. Zabula, *Inorg. Chem.*, 2007, **46**, 7662; (*d*) F. E. Hahn, A. V. Zabula, T. Pape and A. Hepp, *Eur. J. Inorg. Chem.*, 2007, 2405.

7 M. T. Whited, J. Zhang, S. Ma, B.D. Nguyen and D. E. Janzen, *Dalton Trans.*, 2017, **46**, 14757.

8 (*a*) J. C. DeMott, W. X. Gu, B. J. McCulloch, D. E. Herbert, M. D. Goshert, J. R. Walensky, J. Zhou and O. V. Ozerov, *Organometallics*, 2015, **34**, 3930; (*b*) H. Handwerker, M. Paul, J. Blumel and C. Zybill, *Angew. Chem. Int. Ed.*, 1993, **32**, 1313.

9 J. Brugos, J. A. Cabeza, P. García-Álvarez, E. Pérez-Carreño and D. Polo, *Dalton Trans.*, 2018, **47**, 4534.

10 L. Álvarez-Rodríguez, J. Brugos, J. A. Cabeza, P. García-Álvarez, E. Pérez-Carreño and D. Polo, *Chem. Commun.*, 2017, **53**, 893.

11 S. Bestgen, N. H. Rees and J. M. Goicoechea, *Organometallics*, 2018, **37**, 4147.

12 J. A. Cabeza, I. Fernández, J. M. Fernández-Colinas, P. García-Álvarez and C. J. Laglera-Gándara, *Chem. Eur. J.*, 2019, DOI: 10.1002/chem.201902784.

13 L. Álvarez-Rodríguez, J. Brugos, J. A. Cabeza, P. García-Álvarez and E. Pérez-Carreño, *Chem. Eur. J.*, 2017, **23**, 15107.

14 J. Brugos, J. A. Cabeza, P. García-Álvarez and E. Pérez-Carreño, *Organometallics*, 2018, **37**, 1507.

15 (*a*) J. Takaya and N. Iwasawa, *Eur. J. Inorg. Chem.*, 2018, 5012; (*b*) H. Kameo, K. Ikeda, D. Bourissou, S. Sakaki, S. Takemoto, H. Nakazawa and H. Matsuzaka, *Organometallics*, 2016, **35**, 713; (*c*) H. Kameo, K. Ikeda, S. Sakaki, S. Takemoto, H. Nakazawa and H. Matsuzaka, *Dalton Trans.*, 2016, **45**, 7570; (*d*) R. Herrmann, T. Braun and S. Mebs, *Eur. J. Inorg. Chem.*, 2014, 4826; (*e*) H. Kameo, S. Ishii and H. Nakazawa, *Dalton Trans.*, 2012, **41**, 11386.

16 For PGeP germyl complexes in catalysis, see: (*a*) C. Zhu, J. Takaya and N. Iwasawa, *Org. Lett.,* 2015, **17**, 1814; (*b*) J. Takaya, S. Nakamura and N. Iwasawa, *Chem. Lett.,* 2012 ,**41**, 967.

17 See, for example: (*a*) J. M. Goldberg, S. D. T. Cherry, L. M. Guard, W. Kaminsky, K. I. Goldberg and D. M. Heinekey, *Organometallics*, 2016, **35**, 3546; (*b*) T. Liu, W. Meng, Q.-Q. Ma, J. Zhang, H. Li, S. Li. Q. Zhao and X. Chen, *Dalton Trans.* 2017, **46**, 4504.

18 A. F. Kottaus, F. Ballaschk, V. Stakaj, F. Mohr and S. F. Kirsch, *Synthesis*, 2017, **49**, 3197.

19 S. Kumar, G. Mani, S. Mondal and P. K. Chattaraj, *Inorg. Chem.*, 2012, **51**, 12527.

20 (*a*) The average Ge–M distances in Group 11 metal complexes equipped with germyl ligands are 2.35(8) (Cu), 2.46(3) (Ag) and 2.40(5) (Au) Å (CSD version 5.40; updated May 2019); (*b*) See also, F. H. Allen, *Acta Crystallogr. Sect. B*, 2002, **58**, 380.

21 J. I. van der Vlugt, M. A. Siegler, M. Janssen, D. Vogt and A. L. Spek, *Organometallics*, 2009, **28**, 7025.

22 (*a*) G. Kleinhans, M. M. Hansmann, G. Guisado-Barrios, D. C. Liles, G. Bertrand and D. I. Bezuidenhout, *J. Am Chem. Soc.*, 2016, **138**, 15873; (*b*) J.-Y. Hu, J. Zhang, G.-X. Wang, H.-L. Sun and J.-L. Zhang, *Inorg. Chem.*, 2016, **55**, 2274.

23 (*a*) C. R. Wade, T.-P. Lin, R. C. Nelson, E. A. Mader, J. T. Miller and F. P. Gabbaï, *J. Am. Chem. Soc.*, 2011, **133**, 8948; (*b*) H. Yang and F. P. Gabbaï, *J. Am. Chem. Soc.*, 2015, **137**, 13425; (*c*) S. Sen, I.-S. Ke and F. P. Gabbaï, *Inorg. Chem.*, 2016, **55**, 9162; (*d*) S. Sen, I.-S. Ke and F. P. Gabbaï, *Organometallics*, 2017, **36**, 4224.

24 F. Inagaki, C. Matsumoto, Y. Okada, N. Maruyama and C. Mukai, *Angew. Chem. Int. Ed.*, 2015, **54**, 818.

25 F. A. Kotthaus, F. Ballaschk, V. Stakaj, F. Mohr and S. F. Kirsch, *Synthesis*, 2017, **49**, 3107.

26 F. H. Jardine, L. Rule and A. G. Vohra, *J. Chem. Soc. A*, 1970, 238.

27 B.-K. Teo and J. C. Calabrese, *Inorg. Chem*., 1976, **15**, 2467.

28 R. Usón, A. Laguna, M. Laguna, D. A. Briggs, H. H. Murray and J. Fackler, *Inorg. Synth.*, 1989, **26**, 85.

29 M. I. Bruce, B. K. Nicholson, O. B. Shawkataly, J. R. Shapley and H. Henly, *Inorg. Synth*., 1989, **26**, 59.

30 (*a*) *DNMR3*: G. Binsch and D. A. Kleier, SERC NMR Program Library, Daresbury, UK, 1977; (*b*) *DNM3RUN* and *N3PLOT* for Windows: B. W. Tattershall, Newcastle University, Newcastle, UK, 2007.

31 *SPINWORKS*, version 4.2.0: K. Marat, University of Manitoba, Winnipeg, Canada, 2015.

32 *Gaussian 09*, revision D.01: M. J. Frisch, G. W. Trucks, H. B. Schlegel, G. E. Scuseria, M. A. Robb, J. R. Cheeseman, G. Scalmani, V. Barone, B. Mennucci, G. A. Petersson, H. Nakatsuji, M. Caricato, X. Li, H. P. Hratchian, A. F. Izmaylov, J. Bloino, G. Zheng, J. L. Sonnenberg, M. Hada, M. Ehara, K. Toyota, R. Fukuda, J. Hasegawa, M. Ishida, T. Nakajima, Y. Honda, O. Kitao, H. Nakai, T. Vreven, J. A. Montgomery, Jr., J. E. Peralta, F. Ogliaro, M. Bearpark, J. J. Heyd, E. Brothers, K. N. Kudin, V. N. Staroverov, R. Kobayashi, J. Normand, K. Raghavachari, A. Rendell, J. C. Burant, S. S. Iyengar, J. Tomasi, M. Cossi, N. Rega, N. J. Millam, M. Klene, J. E. Knox, J. B. Cross, V. Bakken, C. Adamo, J. Jaramillo, R. Gomperts, R. E. Stratmann, O. Yazyev, A. J. Austin, R. Cammi, C. Pomelli, J. W. Ochterski, R. L. Martin, K. Morokuma, V. G. Zakrzewski, G. A. Voth, P. Salvador, J. J. Dannenberg, S. Dapprich, A. D. Daniels, Ö. Farkas, J. B. Foresman, J. V. Ortiz, J. Cioslowski and D. J. Fox, Gaussian, Inc., Wallingford, CT, 2009.

33 (*a*) A. D. Becke, *J. Phys. Chem. A*, 1988, **38**, 3098; *(b)* J. P. Perdew, *Phys. Rev. B*, 1986, *33*, 8822.

34 F. Weigend and R. Ahlrichs, *Phys. Chem. Chem. Phys*., 2005, **7**, 3297.

35 S. Grimme, J. Antony, S. Ehrlich and H. Krieg, *J. Chem. Phys*. 2010, **132**, 154104.

36 (*a*) J. P. Foster and F. Weinhold*, J. Am. Chem. Soc*., 1980, **102**, 7211; (*b*) A. E. Reed and F. Weinhold, *J. Chem. Phys*., 1985, *83*, 1736; (*c*) A. E. Reed, R. B. Weinstock and F. Weinhold, *J. Chem. Phys*., 1985, **83**, 735; (*d*) A. E. Reed, L. A. Curtiss and F. Weinhold, *Chem. Rev*., 1988, **88**, 899.

37 (*a*) S. Huzinaga and B. Miguel, *Chem. Phys. Lett.*, 1990, **175**, 289; (*b*) S. Huzinaga and M. Klobukowski, *Chem. Phys. Lett.*, 1993, **212**, 260.

38 J. A. Cabeza, J. F. van der Maelen and S. García-Granda, *Organometallics*, 2009, **28**, 3666 and references therein.

39 *AIMAll*, version 19.02.13: T. A. Keith, http://tkgristmill.com.

40 *CrysAlisPro RED*, version 1.171.37.35: Oxford Diffraction Ltd., Oxford, UK, 2014.

41 *SADABS-2016/2*: L. Krause, R. Herbst-Irmer, G. M. Sheldrick and D. Stalke, *J. Appl. Crystallogr.*, 2015, **48**, 3.

42 *SIR-97*: A. Altomare, M. C. Burla, M. Camalli, G. L. Cascarano, C. Giacovazzo, A. Guagliardi, A. G. C. Moliterni, G. Polidori and R. Spagna, *J. Appl. Crystallogr*., 1999, **32**, 115.

43 *SHELXL-2014*: G. M. Sheldrick, *Acta Cryst*., 2008, **A64**, 112.

44 *WINGX*, version 2013.3: J. Farrugia, *J. Appl. Crystallogr*., 2012, **45**, 849.

45 *MERCURY*, CSD version 3.10.1 (build 168220): Cambridge Crystallographic Data Centre, Cambridge, UK, 2018.

Dalton Transactions

ARTICLE

Figure and Text for the Table of Contents

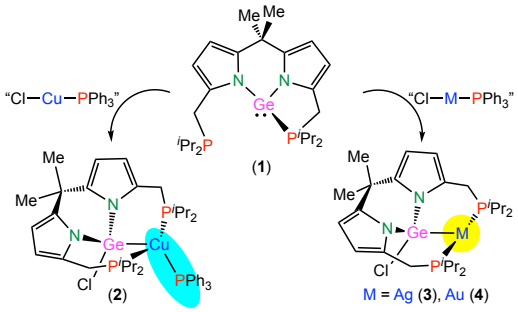

A dipyrromethane-based PGeP germylene has allowed the synthesis of unusual tetrahedral copper(I) and T-shaped silver(I) and gold(I) germyl complexes.